

Mabel Elena Lanfranchini¹⁻²

Ricardo Oscar Etcheverry¹⁻³

Raúl Ernesto de Barrio¹

Clemente Recio⁴

Fontana lake area: a significant precious metal-bearing epithermal target in western Patagonia, Argentina

1- Instituto de Recursos Minerales, FCN y M, UNLP Calle 64 N° 3, (1900) La Plata Argentina

2- Comisión de Investigaciones Científicas de la provincia de Buenos Aires, Argentina

3- Consejo Nacional de Investigaciones Científicas y Técnicas, Argentina

4- Facultad de Ciencias, Universidad de Salamanca, España

E-mail: mlanfranchini@inremi.unlp.edu.ar. Telephone and fax number: 54-221-4225648

Abstract Precious metal-bearing quartz vein occurrences are located throughout the Fontana Lake area in southern Argentina. The mineralization is developed in the Andean continental magmatic arc environment. These deposits and their associated alteration zones are spatially related to a lengthy period of Early Cretaceous calc-alkaline magmatism represented by acid dikes and subvolcanic bodies, and hosted by a Late Jurassic to Early Cretaceous volcano-sedimentary sequence. The veins and related veinlets outcrop discontinuously along a NW-SE belt. The primary mineral assemblage is mainly composed of pyrite ± galena ± chalcopyrite > hematite ± arsenopyrite in silica gangue minerals. Assays of grab samples from selected quartz veins show as much as 5.7 ppm Au and 224 ppm Ag, as well as Pb, Cu, and Zn enrichments. Hydrothermal fluids caused an innermost silicification and adularia-sericite alteration assemblage, and an external propylitic halo.

Sulfur isotope values measured for sulfides (-1.90 to + 1.56‰ $\delta^{34}\text{S}_{\text{H}_2\text{S}}$), and oxygen and deuterium isotopes measured on quartz crystals and extracted primary fluid inclusion waters (-2.85 to -5.40‰ $\delta^{18}\text{O}_{\text{H}_2\text{O}}$, and -113.8 to -10.4‰ $\delta \text{D}_{\text{H}_2\text{O}}$) indicate that mineralization probably formed from magmatic fluids, which were mixed with meteoric waters. Also, fluid inclusion data from quartz veins point out that these fluids had low salinity (1.7 to 4.2 wt% NaCl equiv.), and temperatures of homogenization between 180 and 325°C.

Mineralogical, petrographic and geochemical features for mineralized surface exposures point out a typical adularia-sericite, low sulfidation epithermal system in the Fontana Lake area that represents a very promising target for further exploration programs.

Keywords Precious metal-bearing epithermal occurrence – Patagonia - Argentina

Introduction

Epithermal deposits commonly develop in association with calc-alkaline magmatism in volcanic arcs at convergent plate margins. Many important ore deposits were concentrated around the Pacific Rim during the Cretaceous-Tertiary metallogenic epoch, particularly in the Andean Cordillera of South America. Some of these deposits, such as Huemules (Viera and Hughes 1999), La Ferrocarrilera-Cerro Bayo (Rolando 2001), Arroyo Verde-Arroyo Las Mentas-Mina Angela (Dejonghe et al. 2002), and El Toqui (Wellmer and Reeve 1990), have been well studied in the Argentinean-Chilean part of the Andean Cordillera, but other prospective areas in the region have lacked detailed study. Among these deposits are the epithermal precious metal-bearing quartz veins, and their related alteration zones, in the northeastern part of the Fontana Lake area, southwestern Chubut Province and about 1700 km southwest of Buenos Aires (Fig 1).

Since early last century, the southern sector of Fontana Lake area has been recognized for its conspicuous hydrothermal alteration zones and base and precious metals occurrences. Since then, there have been several exploration projects and research studies in the region.

In the northeastern Fontana Lake area a reconnaissance mapping, digital image processing, field checking, and sampling were undertaken in selected sectors, showing outcrops with veining or with color anomalies. This has led to the discovery of numerous outcrops of quartz veins bearing precious metals, a target now of exploration interest. This paper presents the results of studies at a variety of scales of the precious metal occurrences and the geology of the region where these occurrences crop out. Also, a metallogenic model for this region is presented.

Previous work

Some placer gold deposits were mined in the Fontana Lake area during the beginning of the 20th century, and also the La Ferrocarrilera deposit was mined during the 1950s, but there was no geological information from that activity. Later, metallogenic investigations in the southern part of the Fontana Lake area were carried out by Domínguez (1981) and Rolando et al. (2002), who studied the polymetallic mineralization of the La Ferrocarrilera mine and Cerro Bayo prospect, respectively. Also, regional geologic studies were conducted by Ploszkiewicz and Ramos (1977), Ramos (1981, 1983), and Ploszkiewicz (1987). Between 1990 and 2000, surface exploration work was carried out by mining companies in the Lote 15 (Payaniyeu Range) and the El Abuelo (Pepita Hill) areas. Several resulting targets for the exploration of precious metals were discovered, but to date the results of these studies have not been published. Subsequently, Dejonghe et al. (2002) summarized the metallogenic features of polymetallic mineralization throughout the Chubut province (Arroyo Las Mentas, Arroyo Verde, Calafate, Cañadón Bagual, Huemules, Santa Máxima, La Ferrocarrilera and Angela deposits), and Río Negro province (Gonzalito deposit), and proposed a low sulfidation epithermal classification for the occurrences. Furthermore, these authors compared the mineralization with the gold- and silver-bearing, base metal sulfide-rich quartz veins that were discovered in the Deseado Massif, southern Argentina (Genini 1990), which is currently a metallogenic sub-province with important precious-metal resources.

Folguera et al. (2000) and Folguera and Iannizzotto (2004) proposed a tectonic evolution scheme for the Fontana and La Plata Lakes area. Lanfranchini and Etcheverry (1999), and Lanfranchini (2002) characterized the main geological and metallogenic aspects of the precious metal low sulfidation epithermal veins located in northeastern part of the Fontana Lake area. More recently, Lanfranchini et al. (2007) studied the geology and geochemistry of the El Abuelo calcic Fe-skarn, located in the southern part of the area, a deposit that had been mined between 1940 and 1960.

Regional geological setting

An extensional structural regime characterized the Patagonian Andes during the mid-Late Jurassic to Early Cretaceous. Consequently, a basement block defined by regional NW- and NE-striking subvertical normal faults formed several basins. During this part of the late Mesozoic there was a marine transgression, as well as an episode of intermediate to felsic magmatism, which was associated with formation of precious metal-bearing epithermal quartz veins. The Andean Orogeny subsequently began in the Late Cretaceous and continued through the Tertiary with attendant uplift of the Patagonian Batholith. This was followed by a compressive episode with a WNW main stress direction, as the Nazca Plate was subducted beneath the South American Plate (Sillitoe 1974). This led to reactivation of the existing faults, tectonic inversion, and crustal shortening defined by folding and development of new faults (Folguera et al. 2000; Folguera and Iannizzotto 2004). During the Late Cretaceous, granitic to mafic plutonic rocks were emplaced to form the Patagonian Batholith at the southern end of the Andean Cordillera.

The Lago La Plata Formation is the oldest unit in the study area (Fig 1). It forms small, scarce, isolated outcrops, and it comprises basalt and basaltic andesite of Middle to Late Jurassic age (Ramos 1976). These rocks contain pale green pyroxene and plagioclase (An_{50-52}) phenocrysts, which are enclosed in a groundmass displaying a pilotaxitic texture. The upper part of the volcanic sequence is interlayered with the lower section of the Tres Lagunas Formation, a marine sedimentary succession of Late Jurassic–Early Cretaceous age (Ploszkiewicz and Ramos 1977). The Tres Lagunas Formation is composed of thin greenish sandstone layers interbedded with dark gray pelite and minor limestone. Subsequently, a widely distributed, 1500-m-thick, deltaic sandstone unit, the Apeleg Formation, was deposited (Ploszkiewicz and Ramos 1977). These rocks form tabular thick beds that dip 20°N. This unit comprises light brown, fine to medium size quartz sandstone with a clast-supported texture, and minor conglomerate and pelite.

During the Early Cretaceous, sedimentary processes were interrupted by the spread of rhyolitic to basaltic lava flows and related ash flow tuffs, concomitant with the intrusion of igneous bodies. These magmatic rocks constitute three units: (1) Payaniyeu Formation (Hauterivian-Aptian: Ploszkiewicz and Ramos, 1977) that comprises andesitic to rhyolitic tuffs and ignimbrites, (2) Ñirehuao Formation (Barremian-Aptian: Skarmeta and Charrier, 1976) that is composed of dacitic to basaltic lavas and pyroclastic flows, and (3) El Gato Formation (Aptian-Albian: Ploszkiewicz and Ramos, 1977) that is constituted by dacitic to rhyolitic volcanic to subvolcanic rocks. The Payaniyeu Formation exhibits multicolored elongated and well stratified outcrops. These rocks are composed of a vitroclastic matrix with scarce quartz, feldspar, and biotite. The Ñirehuao volcanic rocks crop out to form rounded hills composed of highly altered greenish to brown andesite with porphyritic texture, where pyroxene and

plagioclase phenocrysts are surrounded by a pilotaxitic groundmass. The El Gato Formation crops out extensively in the study region, constituting widespread lava and ignimbrite flows as well as many dikes and small subvolcanic bodies. These igneous bodies appear as a few kilometer wide hills, constituting the Teta, Pedrero, and Colorado Hills. The predominant NW-striking rhyolitic dikes of the El Gato Formation appear as elongated crests that are 0.5- to 8.0 m-thick and as much as 1000-m-long; they are locally related to a few thin quartz veins and veinlets, with variable strikes. The rhyolitic rocks are light brown in color, and have a porphyritic texture, composed of bipyramidal quartz phenocrysts, as much as 5 mm in length, as well as K-feldspar, plagioclase, euhedral deferrized biotite, and Fe-oxides, with accessory apatite and titanite in a felsitic groundmass.

The Patagonian Batholith is poorly exposed in this region; only a few gabbroic to dioritic rocks (Muzzio Formation, Late Cretaceous: Ramos, 1976) crop out as intrusions within the volcano-sedimentary sequence. These intrusions formed hornfels aureoles in the Del Finadito Hill area and towards the south side of Fontana Lake, near de Bayo Hill (Figs 1 and 2).

Pliocene-Pleistocene basalts and recent glaciofluvial-fluvial deposits complete the stratigraphic column.

Satellite image analysis

A couple of scenes of ascending and descending orbits of a georeferenced RADARSAT SAR image, with fine resolution, 37-40° angle of incidence, a pixel spacing of 6.25 meters in both azimuth and coverage, and a resolution of image 10 x 10 meters were used. This image was rectified using a LANDSAT-TM Image and aerial photographs. Enhancement and contrast linear features were performed by conventional treatments.

In the Fontana Lake area, satellite image analysis allowed us to identify color alteration zones and several linear morphological features with positive topographic expression (Marchionni et al. 1997; Marchionni et al. 1999). These features mainly correspond to areas of mineralized rhyodacitic dikes and surrounding hydrothermal alteration zones. These linear structures have been effective tools as exploration guides in the study area. The main mode of these lineaments shows a marked NW-trending direction and a subordinate NE-striking orientation. This structural scheme is consistent with that proposed by Ploszkiewicz and Ramos (1977), which suggested the lineaments defined boundaries of block-faulting of the crystalline basement. The continuation of the lineaments into younger sedimentary rocks indicates a reactivation of the normal faults during very recent times.

Vein deposits

Epithermal quartz veins occur in several places of the Payaniyeu region within the Late Jurassic-Early Cretaceous volcano-sedimentary sequence. They are spatially related to the intrusion of rhyolitic and rhyodacitic dikes of the El Gato Formation. Although the quartz veins constitute discontinuous outcrops, their crest morphology shows a sinuous outcrop pattern that generally trends NW-SE in an approximately 30-km-long by 15-km-wide belt. These veins are near vertical, they are a few centimeters to several

meters thick, and tens to hundreds of meters long. The main veins contain some anomalous values in precious and base metals (Table 1).

The principal quartz veins crop out at the Lote 15 sector in the Payaniyeu Range (Figs 1b and 3) and at the Mina de Plomo sector in the Sakmata Cordillera (Figs 1a and 2). They are near vertical, and have N 30-40° W and minor N 50° E (Mina de Plomo) strikes. The veins crop out discontinuously for almost 900 m, they are as much as 5-m-wide and are commonly hosted by rhyodacitic dikes of the El Gato Formation, which are intruded into the volcano-sedimentary succession. The immediate wall rocks to the vein system, constituted mainly by rhyodacite, andesite and sedimentary rocks, have been altered to a quartz-sericite assemblage, and are locally brecciated and cut by microcrystalline quartz veins (Fig 4). This alteration extends for at least 15 m from the veins, where it grades outward to a propylitic assemblage.

Banded and breccia textures are developed surrounding rhyodacite and andesite wall rock fragments, each a few centimeters in diameter, that are located near both the centers and the margins of the quartz veins (Figs 5 a and b). The veins are composed of milky to translucent quartz with lesser sparitic spathic carbonate. Quartz presents mostly massive, zoned crystals and comb primary textures (Figs 5 c and d); also, evidence of recrystallization includes mosaic and flamboyant textures. In addition, several cross-cutting thin quartz veinlet systems occur throughout the mineralized zones.

The hypogene mineral assemblage is composed of pyrite ± galena ± chalcopyrite > hematite ± arsenopyrite ± chlorite ± fluorite ± rutile, with variable amounts of gold and silver. Gold appears as minute native mineral grains as long as 10 µm or as micro-inclusions in the sulfide minerals. Pyrite appears as different generations of crystals, which show euhedral square sections, as much as 5 mm in diameter. It occurs either disseminated in quartz veins or in the adjacent wall rocks, commonly oxidized to boxworks. Galena occurs as fresh 3 cm in diameter grains, and frequently contains chalcopyrite exsolutions. It is sometimes partially replacing pyrite crystals and it is intergrown with quartz grains. Chalcopyrite is scarce and erratically distributed as irregular masses with anhedral 2 mm in diameter crystals. In polished sections, hematite is observed as inclusions in pyrite or in the gangue minerals as lamellas as much as 500-µm-long or forming radiated aggregates. Arsenopyrite appears occasionally as 400-µm-long euhedral rhombic sections. Also, chlorite, needle-like rutile, and fluorite are present in minor amounts filling pores and small fractures.

Several stockworks and quartz veinlets, that also contain sulfide minerals, are 0.3- to 0.8-cm-wide, almost parallel to the main veins, and also cut the Early Cretaceous volcanic rocks. The edges of these mineralized zones are quite clear and are marked by euhedral pyrite and dark brown limonite. In addition, numerous, very thin quartz-epidote-chlorite-sericite stringers are frequently present in the zones.

A thin supergene zone was developed along the main mineralized structures. These are marked by a very colorful mineral assemblage comprising secondary sulfides (covellite, chalcocite), and oxides (anglesite, cerusite, and Fe-oxides) in thin veinlets, and particularly replacing hypogene chalcopyrite and galena grains.

In the Teta Hill area (Fig 6), several near vertical quartz lodes, each as much as 5-m-wide, strike approximately E-W. At Colorado Hill, the veins have similar features but a variable strike between N-S

and NW-SE. Despite there are no visible sulfides in the outcrops of milky quartz, geochemical analyses reveal as much as 524 ppb Au and 76 ppm Ag.

The general mineral paragenetic sequence shows the following main stages: (1) earliest generation of euhedric pyrite crystals that precipitated before the main generation of cubic galena. Between these mineralizing events, chalcopyrite appears as irregular grains sometimes included in galena crystals; (2) after the galena deposition, a second pyrite cubic crystals were formed; (3) the sequence ends with a late stage of disseminated fine pyrite, mainly located towards the edge veins and the adjacent wall rocks.

Two hydrothermal quartz vein systems related to a Ca-Fe-magnetite skarn (Lanfranchini et al. 2007), named El Abuelo, and El Solcito, are located at Pepita Hill, in the southern part of the study area. Ore grades vary between 40 and 63 wt% Fe, and, in addition, anomalous metal contents of >1% Cu and as much as 81 ppm Ag have been measured.

Hydrothermal alteration

Narrow hydrothermal alteration zones surround the mineralized veins. Silicification, the most pervasive alteration, is best developed in the sandstone of the Apeleg Formation; it is much less extensive in the andesitic rocks. Silicification is evident both as a pervasive texture composed of minute quartz and chalcedony grains, and as very thin veinlets that are accompanied by minor sericite patches. Within these veinlets, minor amounts of euhedral rhombic adularia crystals, as much as 350 μm in length, and anhedral quartz crystals appear intergrown. Sericite is frequently disseminated in the wall rock forming small patches, as well as scarce, 50 μm to 1 mm in diameter, xenomorphic grains of pyrite. Veinlet walls are locally coated with radiated or iron oxide tinted sericite.

Argillically altered rocks are not easily recognized because they are frequently buried by thin Quaternary detrital cover. They are poorly developed adjacent to many of the veins for a few meters into the wall rocks. Argillic alteration is mainly identified in feldspars that show moderate breakdown to kaolinite.

Distal to the veins, mainly in the andesitic flows of the Ñirehuao Formation a strong propylitic alteration is defined by dark grayish-greenish, rock several meters in width. In thin sections, it is observed that calcite and epidote replace plagioclase, and chlorite replaces pyroxene.

Geochemical analyses

Many representative quartz veins and altered wall rocks were studied, and sampled for whole rock geochemical analysis in order to detect the presence of metal anomalies. Minor and trace element contents were analyzed for 63 selected samples by inductively coupled plasma–mass spectrometry (ICP-MS), and by instrumental neutron activation analysis (INAA) at Actlabs Ltd. (Canada).

Electron microprobe analyses were carried out on sulfide minerals with the aim of establishing anomalous contents of precious metals, using a Cameca Camebax SX-50 at the Departamento de Geología, Universidad de Oviedo, Spain. Operating conditions were a 15 to 20 kV accelerating voltage,

beam current of 15 to 20 mA, and beam size of 1 to 2 μm . Natural standards were certificated by MAC (Micro Analysis Consultants Ltd., United Kingdom).

Geochemical analyses on surface grab samples from the principal quartz veins reveal anomalous values in precious and base metals. The highest precious metal contents were found at the Lote 15 and Mina de Plomo occurrences, where Au values are as much as 5.7 and 1.6 ppm, and Ag is as much as 26.5 and 223.8 ppm, respectively (Table 1). The highest Au and Ag values correlate moderately with Fe-Pb>Cu>Zn at Lote 15 and Mina de Plomo, which are consistent with the abundance of recognized sulfide minerals. Also, other pathfinder element enrichments like As, that reaches as much as 429 ppm, Sb (46 ppm) and Hg (110 ppb) correlate with the main Au and Ag values.

Complementary electron microprobe analyses performed on pyrite, galena, and chalcopyrite crystals reveal anomalous Au and Ag contents (as much as 0.15 and 0.31 atomic percent, respectively) that are probably due to submicroscopic inclusions. Also, Au correlates weakly with As at the Lote 15 and Mina de Plomo occurrences.

Fluid inclusions

Methodology

Fluid inclusion heating and freezing analyses were obtained on approximately 50- to 100- μm -thick doubly polished rock-thin sections using a LINKAM THM SG 600 heating-freezing stage in the Fluid inclusion Laboratory at the Centro de Desenvolvimento de Tecnologia Nuclear, Belo Horizonte, Brazil and at the Instituto de Recursos Minerales, Universidad Nacional de La Plata, Argentina. Calibration with standards of known melting points indicates an accuracy of $\pm 2^\circ\text{C}$ for liquid-vapor homogenization on heating and $\pm 0.5^\circ\text{C}$ for freezing point depressions. Low temperature phase changes were measured first in order to minimize the possibility of inclusion decrepitation. The samples were initially cooled to -120°C , and then slowly warmed with the purpose of measuring first melting (T_c) and final melting (T_m) temperatures. Further heating allowed the determination of liquid-vapor homogenization temperatures (T_h).

Petrography

Different textural varieties of euhedral to subhedral quartz crystals were studied for fluid inclusions (FI). Eighteen quartz samples from the Lote 15 and Mina de Plomo occurrences in the Payaniyeu Range were examined to estimate the temperature and composition of hydrothermal fluids. Quartz from the main veins and silicified wall rocks contained zones of primary FI, and planes of secondary and pseudosecondary FI. Primary FI data from euhedral, 1- to 3-cm-long quartz crystals, which are intergrown with sulfide grains and small rhombic adularia crystals of 90 μm average length, were analyzed. These quartz crystals contain growth zones (Fig 7) mainly defined by abundant two-phase FI, as well as a few small monophase (<5 μm) primary FI that are not suitable for microthermometric analysis. Primary FI also occur as isolated clusters in these crystals. Pseudosecondary and secondary FI

are distributed along healed and late fissure planes; no microthermometric analyses were performed on them.

Primary two-phase FI ($L_{H_2O}+V_{H_2O}$) range between 10 and 50 μm in size. They have irregular, almost polygonal, elongated shapes, occasionally showing “necking down” features. Vapor phase volume varies from 10 to 20% of total FI volume (Fig 7). Locally, some groups of primary FI exhibit variability from 10 to 50% in vapor phase volumes. Although these FI have different proportions of vapor phase, they homogenize at the same temperature.

Microthermometric measurements

Microthermometric measurements were restricted to quartz-hosted inclusions because the inclusions could be assigned a primary origin, and the inclusions are large and easy to observe. During the first freezing measurements in both studied vein systems, no phase changes occurred that indicated the presence of carbon-bearing volatile phases in the vapor. The fluid inclusions had first melting temperatures (T_c) between -22 and -24°C , similar to the eutectic for the system $\text{NaCl} - \text{H}_2\text{O}$, with minor K^+ that would have been responsible for the depletion of the eutectic point of the system below the theoretical -20.8°C (Shepherd 1985). The final melting temperatures (T_m) for ice range between -2.5°C and -1°C , indicating low salinities that vary between 1.7 and 4.8 wt % NaCl equiv., with a mode in the range of 3.5 - 4.5 wt % NaCl equiv. (Fig 8, Table 2).

During heating experiments, the two-phase FI homogenized into the liquid phase at temperatures between 180°C and 300°C , with two modes at $200^\circ - 220^\circ\text{C}$ and $260^\circ - 280^\circ\text{C}$, with the first corresponding to the FI in the peripheral sectors of crystals, whereas the second mode corresponds to the cores (Fig 8).

Stable isotope studies

Representative samples of silicates and sulfides were selected for stable isotope determinations and these were performed at the Laboratorio General de Isótopos Estables, Facultad de Ciencias, Universidad de Salamanca, Spain. Extracted gasses were analyzed in a VG Isotech micromass SIRA-II spectrometer, equipped with a cryogenic system (“cold finger”). The measured isotopic ratios were reported in the conventional delta notation (δ ‰). Oxygen and hydrogen gas extractions were performed by conventional methods (Clayton and Mayeda 1963) in a fluorine line. Also, O and H isotope fractionation was determined through the fluids extracted from primary fluid inclusions hosted in quartz crystals by the method of decrepitation. The isotope ratios are given relative to the Standard Mean Ocean Water (SMOW), with an analytical error of ± 0.8 ‰ for $\delta^{18}\text{O}$, and ± 1 ‰ for δD . SO_2 gas extraction from sulfide samples (galena and pyrite crystals) was performed by conventional methods (Robinson and Kusakabe 1975). Sulfur compositions are reported in delta notation relative to the CDT standard ($\delta^{34}\text{S}$), with an analytical error of ± 0.27 ‰.

Stable isotope (O, H, S) data are summarized in Table 3. The $\delta^{18}\text{O}_{\text{H}_2\text{O}}$ values were calculated from isotopic measurements on quartz crystals from Lote 15 veins, using the fractionation equations of Zheng (1993) at 280°C , as based on the FI data. Moreover, $\delta\text{D}_{\text{H}_2\text{O}}$ and some $\delta^{18}\text{O}_{\text{H}_2\text{O}}$ data were measured directly

from the extracted fluid phase of primary fluid inclusions in quartz crystals, as there were limited coarse hydroxyl-bearing minerals for δD_{H_2O} determination. The fluid was obtained by decrepitation of primary fluid inclusions, hosted in quartz crystals with only one generation of FI. The fluid extraction was done in a tubular oven, under controlled temperature and with a small decrepitation temperature range. There is always concern over the reliability of δD analyses in fluids obtained by decrepitation methods, due to possible contamination of the primary fluid δD values by fluids from secondary inclusions that were unrelated to the vein-forming event. However, our results seem reliable because they show consistency between analyses and because the $\delta^{18}O_{H_2O}$ results obtained using both decrepitation of FI and quartz crystals were identical. The samples analyzed were those that had been in contact with sulfides throughout the exposed vein system; these sulfides comprise less than about 1 percent of the total vein, but their isotopic composition is nevertheless genetically significant.

The $\delta^{18}O_{H_2O}$ measurements range between 5.3 and 5.4 ‰ in quartz crystals, -2.85 and -0.91‰ in fluid inclusions of quartz, whereas, δD_{H_2O} yielded values of -106.4 to -103.4‰ in fluid inclusions of quartz crystals. Reference meteoric waters, employed to infer metallogenic environment, were determined from the pluviometric data base of the International Atomic Energy Agency (Vienna). These waters are considered to have similar paleolatitude, altitude, and continental conditions to those during the Cretaceous (Fig 9).

Sulfide sulfur isotopes ($\delta^{34}S_{min}$) from the Lote 15, Pepita hill (El Abuelo skarn and El Solcito vein), and Mina de Plomo quartz veins and veinlets, yielded values from -1.90‰ to +1.56‰ (Table 3). The $\delta^{34}S_{H_2S}$ was recalculated using the fractionation equations of Ohmoto and Rye (1979), at 300°C.

Stable isotope thermometry

Oxygen isotope systematics were used to get an independent estimate of vein formation. The measured quartz and fluid phase extracted from quartz crystal pairs give vein temperatures of about 265°C, using experimental coefficients from Clayton et al. (1972). This agrees very well with the range of 220 to 280°C estimated from fluid inclusion for the quartz deposition.

Sulfur isotope thermometry was attempted without much success on pyrite-galena pairs. Galena intergrowths seem as if they could be reliable, but even these do not meet paragenetic criteria for equilibrium deposition very well. Similarly, in rare pyrite-galena contact associations, the galena involved is a young generation overgrown on older pyrite. Of all the examined associations, only two (samples P8, and 1187) seem to have both sulfides as products of the same paragenetic stage and, even in these, the pyrite appears somewhat older. These samples give $\delta^{34}S_{py} - \delta^{34}S_{ga}$ values correlative with equilibrium temperatures in the range of 340 to 480°C (from the equations of Ohmoto and Rye, 1979, and Li and Liu, 2006), clearly in contradiction to the fluid inclusion data. We infer that these two carefully selected specimens represent non-equilibrium phases, probably as a result of non-contemporaneous deposition.

Discussion

Precious metal-bearing quartz vein formation in the Fontana Lake area occurred immediately after the intrusion of the Early Cretaceous igneous bodies into the Late Jurassic to Early Cretaceous volcano-sedimentary sequence. These vein deposits extend mainly along a N30°/60°W direction, suggesting a structural control for the circulation of hydrothermal fluids through previous faults that were reactivated late in the Cretaceous. These vein systems formed at relatively high levels; the depth at which they formed can be inferred from fluid inclusion data, considering that they were trapped during boiling processes and therefore do not require a pressure correction (Haas 1971; Bodnar et al. 1985). Indirect evidence for such boiling is the existence of some groups of primary FI with different proportions of vapor phase that homogenized at the same temperature (Fig 10). Pressures of about 60-70 bars can be calculated for these solutions, from data obtained for the NaCl-H₂O system, assuming <5 wt% NaCl equiv. salinity, a density of 62-65 g/cm³, and an upper limit of the temperature of homogenization of about 280°C. Under hydrostatic conditions, these pressures should be equivalent to a maximum depth of 750 m below the paleosurface. In addition, the presence of quartz and chalcedony, with lesser adularia and carbonate, the occurrence of distinctive vein textures, including colloform and crustiform banding and comb quartz, and the low temperature FI that lack detectable CO₂, also suggest a high level of emplacement.

A magmatic origin for the sulfur in the vein-forming fluids is assumed due to the close spatial relationship between the rhyolitic to dacitic subvolcanic bodies and the quartz veins, as well as by the sulfur isotope data. The samples analyzed are reasonably representative of sulfides throughout the exposed vein system. Sulfide minerals show a very narrow range of $\delta^{34}\text{S}$ values from -1.90 to +1.56 per mil. This tight range indicates that the sulfides were deposited from hydrothermal solutions whose sulfur was derived from a single source. These hydrothermal fluids may have derived their sulfur directly from magma or from the leaching of sulfides in igneous host rocks.

The $\delta^{18}\text{O}_{\text{H}_2\text{O}}/\delta\text{D}_{\text{H}_2\text{O}}$ diagram (Fig 9, after Sheppard 1986) shows there are two possibilities for the origin of the water: (1) water was derived from a magmatic system and probably mixed with meteoric waters, or (2) meteoric waters formed the veins, but with some interaction of fluids with the country rocks such that they could have incorporated heavier oxygen into the fluids. The meteoric waters likely descended along high-angle normal faults, and (or) the porous and permeable sedimentary country rocks. The extent of exchange of water is not really known, as there are diverse processes that change the isotopic composition of a hydrothermal water.

In addition, fluid pressure decreased during the hydrothermal fluid upwelling causing its partial degassing, and consequently pH increase, through H₂S loss, during short periods of boiling. These facts can be supplemented by the presence of rhombic adularia in quartz veins that is very common in areas of boiling geothermal systems, because a pH increase favors the precipitation of that feldspar. This increase in pH could also have favored base metal sulfide precipitation. Consequent sulfur depletion in the hydrothermal fluids could have broken Au and Ag bisulfide complexes, resulting in the precipitation of precious metals together with sulfides (Reed and Spycher 1985).

An intrusion-related model of this epithermal deposits is schematically shown in Figure 11, through cross sections that illustrate the metallogenic evolution at Fontana Lake area during the Mid-Upper Jurassic to Lower Cretaceous, beginning with the volcanic arc formation, followed by a sedimentary

sequence deposition and by the emplacement of rhyolitic bodies and related quartz veins. Fluid flow patterns are indicated with arrows.

Conclusions

Widespread calc-alkaline magmatism, part of a N-S volcanic arc, occurred during the Jurassic - Early Cretaceous in southwestern South-America. In the Fontana Lake area, this igneous activity formed several intrusive bodies and dikes that are spatially and genetically associated with precious metal-bearing low sulfidation epithermal systems. This magmatism represents a useful guide for explorationists because it is linked to a broad area of mineralization described in this paper.

Although in Fontana Lake area existing knowledge of these epithermal deposits is limited, particularly due to limited drilling to define deeper levels, our surface geological studies allow some generalizations. These include: (1) the presence of a regional geochemical signal, with enrichment of Au, Ag, As, and Hg, (2) a widespread epithermal vein distribution that forms a 450 km² area, and (3) several textural features that point out relatively high to moderately high level of development. Existing geochemical data suggest the presence of both silver-rich and more gold-rich vein systems in the area. These geological features encourage the implementation of further exploration programs in the region.

Acknowledgments This work was financially supported by the Consejo Nacional de Investigaciones Científicas y Tecnológicas of Argentina (CONICET-PIP 2727). The microprobe analyses have been carried out with the assistance of Dr. Agustín Martín-Izard in the Departamento de Geología, Universidad de Oviedo, Spain and the FI measurements with the support of Dr. Francisco J. Ríos in the Centro de Desenvolvimento de Tecnologia Nuclear, Belo Horizonte, Brazil. We are very thankful for the kind and constructive help of Richard Goldfarb.

References

- Bodnar RJ, Reynolds TJ, Kuehn CA (1985) Fluid Inclusions systematics in the epithermal systems. In: Berger A and Bethke P (eds) *Geology and Geochemistry of epithermal systems*, *Reviews in Econ Geol* 2:73-97
- Clayton R, Mayeda T (1963) The use of bromine pent fluoride in the extraction of oxygen from oxides and silicates for isotopic analysis. *Geochim Cosmochim Acta* 27:43-52
- Clayton R, O' Neil J, Mayeda T (1972) Oxygen isotope exchange between quartz and water. *J Geophys Resour* 77:3057-3067
- Dejonghe L, Darras B, Hugues G, Muechez P, Scoates J, Weis D (2002) Isotopic and fluid – inclusion constraint on the formation of polymetallic vein deposits in the central Argentinian Patagonia. *Miner Depos* 37:158-172
- Domínguez E (1981) Génesis y geoquímica de la mineralización de los Yacimientos "Los Manantiales" y "Lago Fontana", prov. del Chubut. *Rev Asoc Geol Argent* 36:123-142

- Folguera A, Vieiro J, Gómez A (2000) Evolución Geológica de los Andes, del Lago La Plata (45° S). IX Congr Geol Chil II:197-200 Puerto Varas
- Folguera A, Iannizzotto NF (2004) The Lagos La Plata and Fontana fold- and thrust- belt: long lived Orogenesis at the edge of western Patagonia. *J South Amer Earth Sci* 16:541-566
- Genini AD (1990) Cerro Vanguardia, provincia de Santa Cruz, nuevo prospecto auro-argentífero. III Congr Nac Geol Econ 3:A97-A110 Olavarría
- Hass J jr. (1971) The effect of salinity on the maximum thermal gradient of a hydrothermal system of hydrostatic pressure. *Econ Geol* 66:940-946
- Lanfranchini ME (2002) Rasgos geológicos y metalogénesis de la Sierra de Payaniyeu y sus alrededores. Provincia del Chubut. Argentina. Facultad de Ciencias Naturales y Museo, Universidad Nacional de La Plata, 771, 222 p. Unpublished Doctoral Thesis
- Lanfranchini M, Etcheverry R (1999) "Lote 15", Manifestación epitermal en Estancia Pepita, Provincia del Chubut. In: Zappettini E (ed) Recursos Minerales de la República Argentina, SEGEMAR An 35:1161-1165
- Lanfranchini ME, de Barrio RE, Etcheverry RO (2007) El Abuelo calcic Fe-skarn, Chubut Province, Southern Argentina. *Explor Min Geol*. In: Richards J and Lentz D (eds) 16:145-158
- Marchionni D, Lanfranchini M, de Barrio R, Schalamuk I (1997) Prospección de dépôts minéraux polymétalliques dans la zone du Lac Fontana, Province de Chubut, Argentina. Utilisation de images SAR de RADARSAT por L'analyse lithologique et structurale. 439 (CD-ROM). Intern Symp Geomat Era Radarsat, Ottawa
- Marchionni D, Lanfranchini M, Schalamuk I, Etcheverry R (1999) Aportes de la información SAR de RADARSAT al estudio Geológico – Metalogénico de la Sierra de Payaniyeu, sector norte del Lago Fontana, Provincia del Chubut, (Argentina). Globesar II Final Symp RadarSat Appl Latin Am. Buenos Aires
- Li YB, Liu JM (2006) Calculation of sulfur isotope fractionation in sulfides. *Geochim Cosmochim Acta* 70:1789-1795
- Ohmoto H, Rye R (1979) Isotope of sulfur and carbon. In: Barnes H (ed) *Geochemistry of Hydrothermal deposits*. John Wiley & Sons pp 509-567
- Ploszkiewicz J (1987) Descripción Geológica de la Hoja 47 c, Apeleg, Provincia del Chubut. *Dir Nac Miner Geol, Bol* 204 pp 1-100
- Ploszkiewicz J, Ramos V (1977) Estratigrafía y Tectónica de la Sierra de Payaniyeu (Provincia del Chubut) *Rev Asoc Geol Argent* 32:209-226
- Ramos V (1976) Estratigrafía de los Lagos Fontana y La Plata (Chubut), Argentina. I Congr Geol Chil I (A):43-64
- Ramos V (1981) Descripción geológica de la Hoja 47 a b "Lago Fontana". Provincia del Chubut. *Serv Geol Nac, Bol* 183 pp 1-143
- Ramos V, 1983. Evolución Tectónica y Metalogénesis de la Cordillera Patagónica. II Congr Nac Geol Econ I:107-124
- Reed, M. & Spycher, N. (1985) Boiling, cooling and oxidation in epithermal systems: a numerical modeling approach. *Reviews in Econ Geol* 2:249–272

- Robinson BW, Kusakabe M (1975) Quantitative preparation of sulfur dioxide for $^{34}\text{S}/^{32}\text{S}$ analyses from sulfides by combustion with cuprous oxide. *Analytical Chem* 47:1179-1181
- Rolando AP (2001) Metalogenia de metais base e evolucao cristal da regio do Lago Fontana, Andes Patagônicos, Argentina. Universidade Federal Rio Grande do Sul, Brasil. Unpublished Doctoral Thesis
- Rolando P, Hartmann L, Santos J, Fernández R, Etcheverry R, Schalamuk I, Mc Naughton N (2002) Mesozoic evolution of the Lago Fontana magmatic arc, Patagonian Andes, based on zircon U-Pb SHRIMP geochronology. *J South Amer Earth Sci* 15:267-283
- Shepherd T (1985) A practical guide to Fluid Inclusions Studies. In: Blackie J (ed) pp 1-239
- Sheppard S (1986) Characterization and isotopic variations in natural waters. Stable Isotopes in High Temperature Geological Processes. *Reviews in Mineralogy*. In: Valley J, Taylor H and O' Neal J (eds) 16:165-183
- Sillitoe RH (1974) Tectonic segmentation of the Andes: implication for magmatism and metallogeny. *Nature*, 250:542-545. London
- Skarmeta J, Charrier R (1976) Geología del sector fronterizo de Aysen entre los 45° y 46° de latitud sur, Chile. VI Congr Geol Argent I:267-286
- Viera RLM, Hughes G (1999) El yacimiento polimetálico aurífero Huemules, Chubut. In: Zappettini EO (ed) Recursos Minerales de la República Argentina. Serv Geol Miner Argent, An 35:1369-1376 Buenos Aires
- Wellmer F, Reeve E (1990) The Toqui Zinc - Lead - Copper - Silver Deposits, Aysén Province Chile. *Stratabound Ore Deposits in the Andes*. Springer Verlag, Berlín Heidelberg pp 473-484
- Zheng Y (1993) Calculation of oxygen isotope fractionation in anhydrous silicate minerals. *Geochim Cosmochim Acta* 57:1079-1091

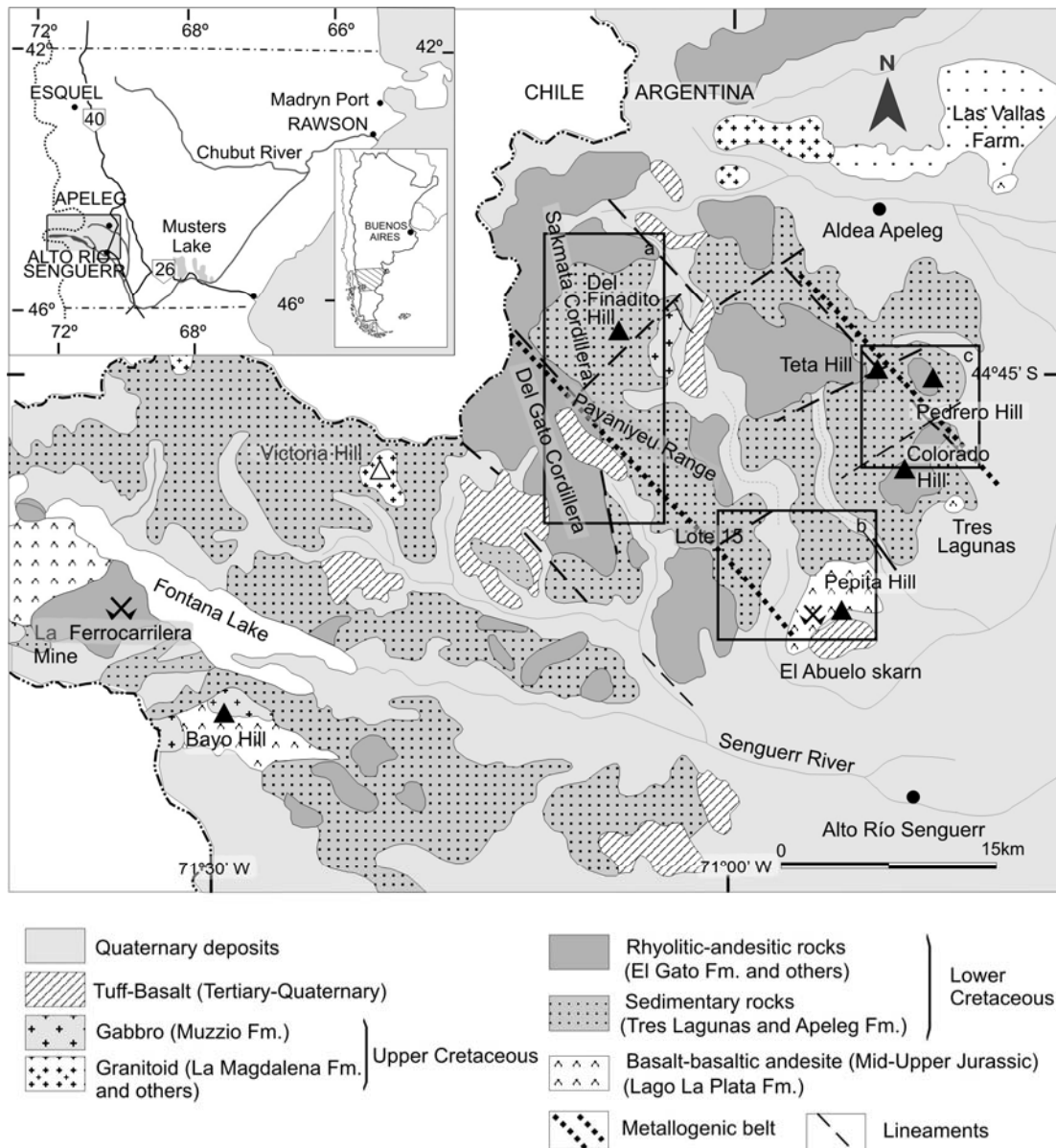


Fig. 1 Regional geology of the northeastern sector of the Fontana Lake area and surrounding zones. Main study areas are marked with rectangles, and named as follows a) Area of figure 2 that includes the southern portion of Sakmata Cordillera, b) Area of figure 3, and c) Area of figure 6

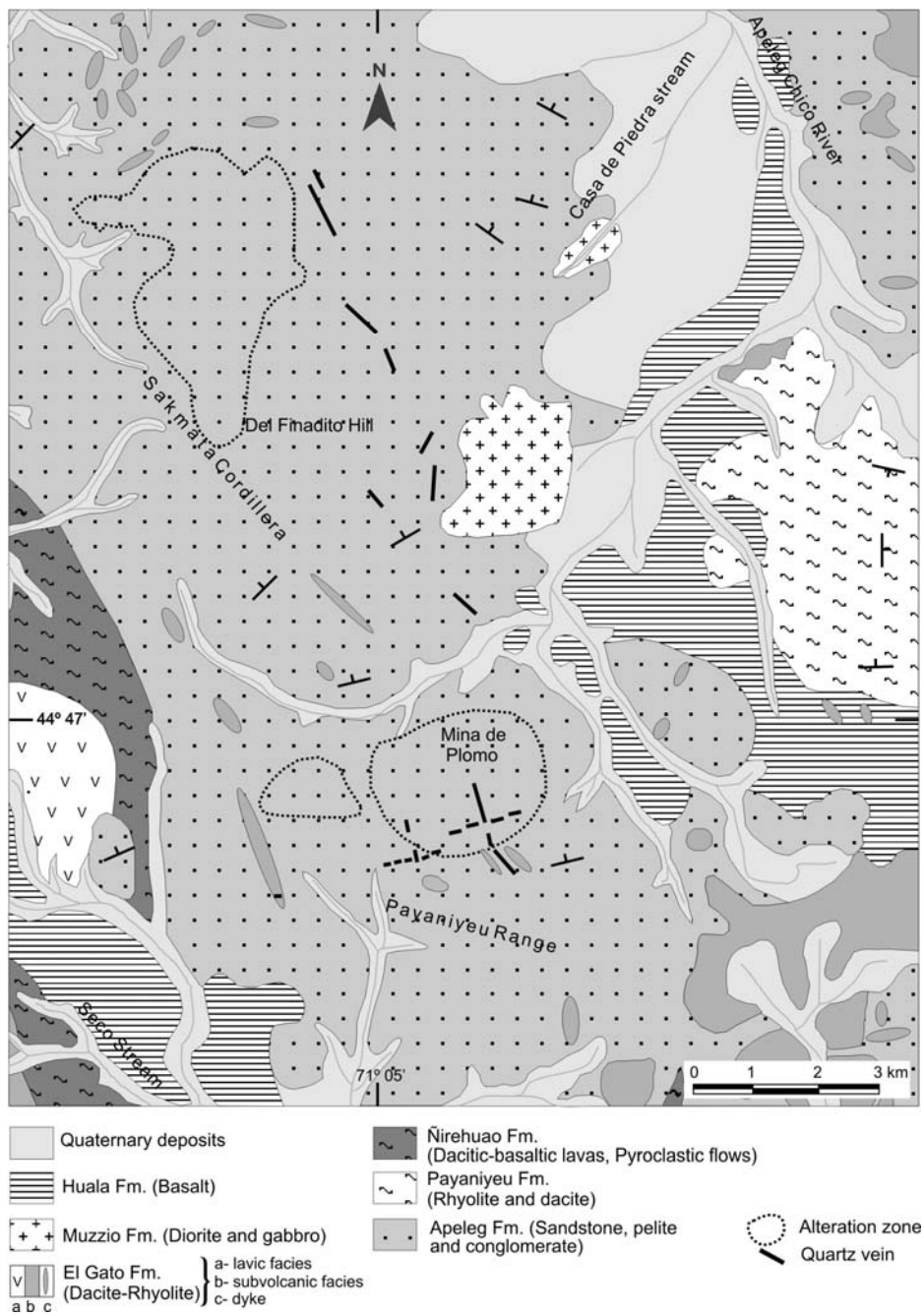


Fig. 2 Geologic map of the Sakmata Cordillera, and the northern part of Payaniyeu Range

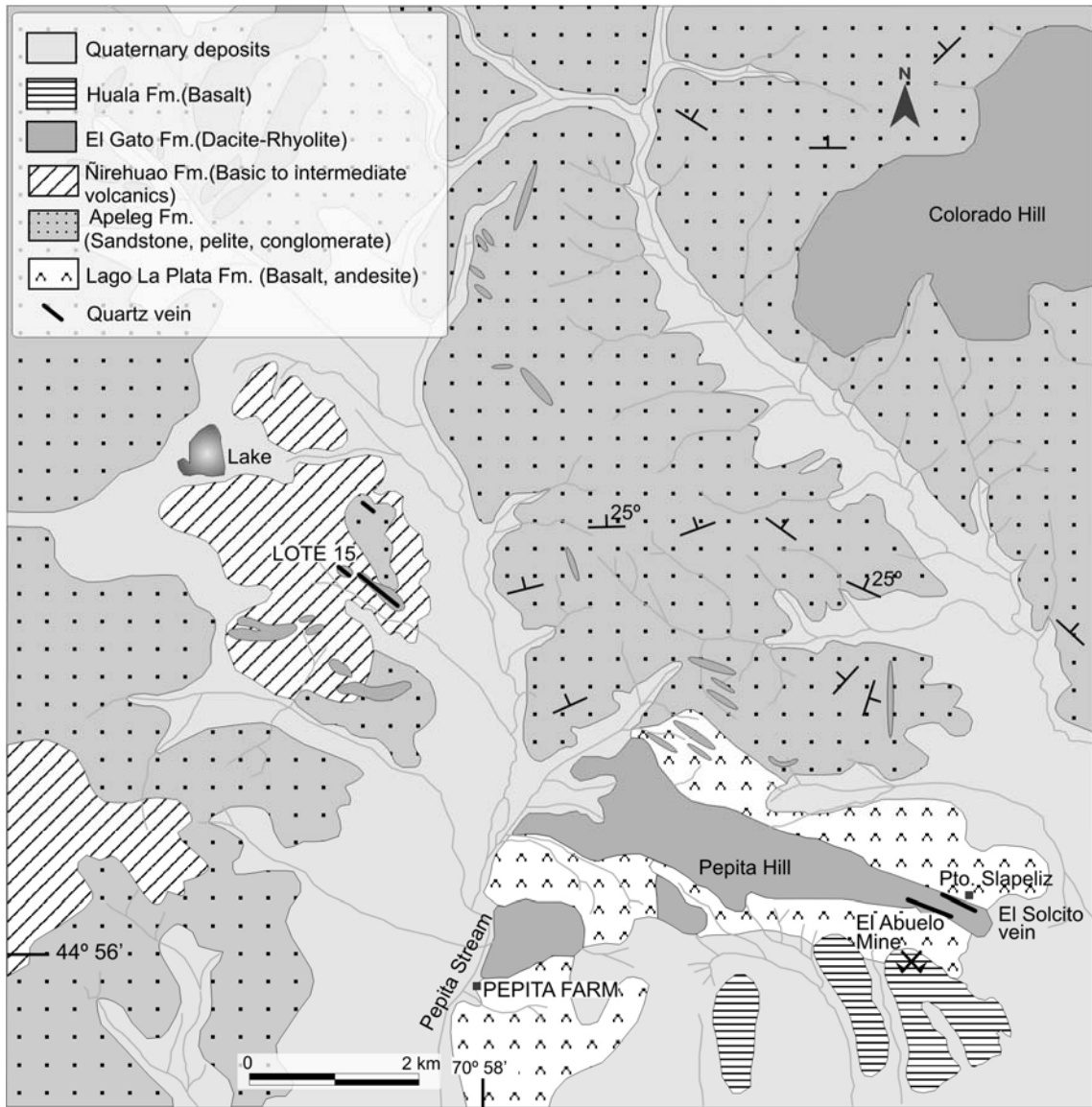


Fig. 3 Geologic map of the southern sector of the Payaniyeu Range, and Pepita Hill

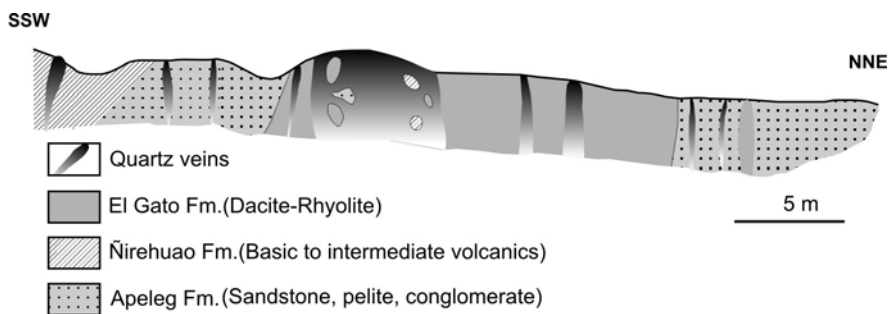


Fig. 4 Schematic cross section showing through the Lote 15 mineralized structure (not to scale)

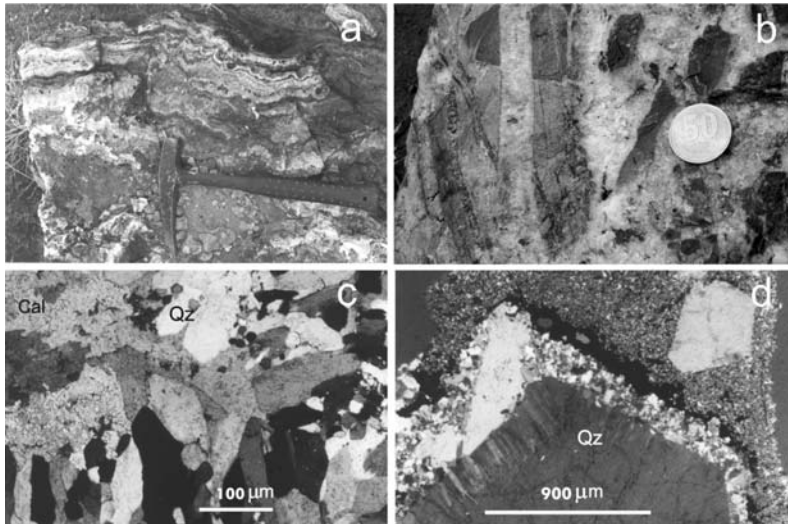


Fig. 5 **a** Field photograph showing quartz-chalcedony banded texture in Lote 15 sector, Payaniyeu Range. **b** Hand specimen photograph of breccia texture from Pepita Hill, coin size 25 mm. **c-d** Textures of quartz in Lote 15 sector (photomicrographs): **c** comb and mosaic textures, and **d** zoned quartz crystal with flamboyant texture towards the rim

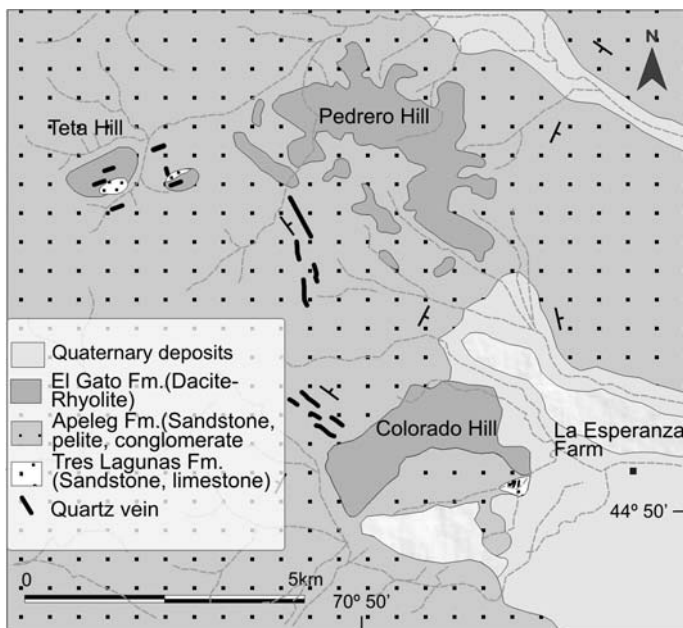


Fig. 6 Geology of the Teta, Colorado, and Pedrero Hills

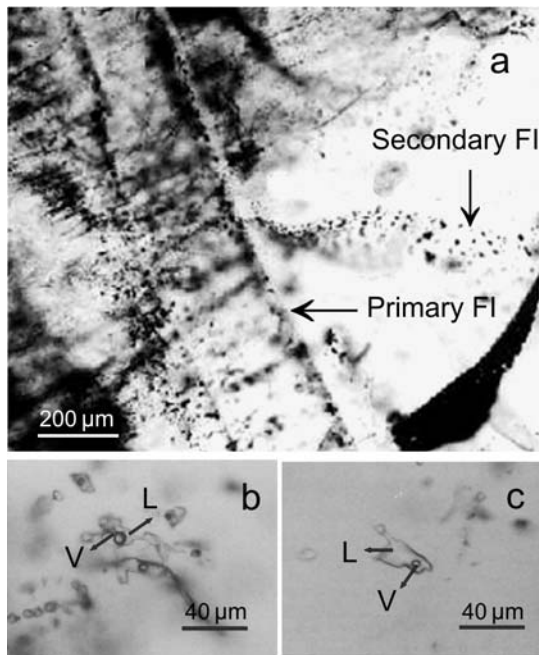


Fig. 7 Photomicrographs of FI in vein quartz, Lote 15, Payaniyeu Range. **a** Quartz crystal showing secondary and primary fluid inclusions along healed fracture planes and growth planes, respectively. **B** and **c** Close-up of previous photograph showing L (liquid) rich primary FI

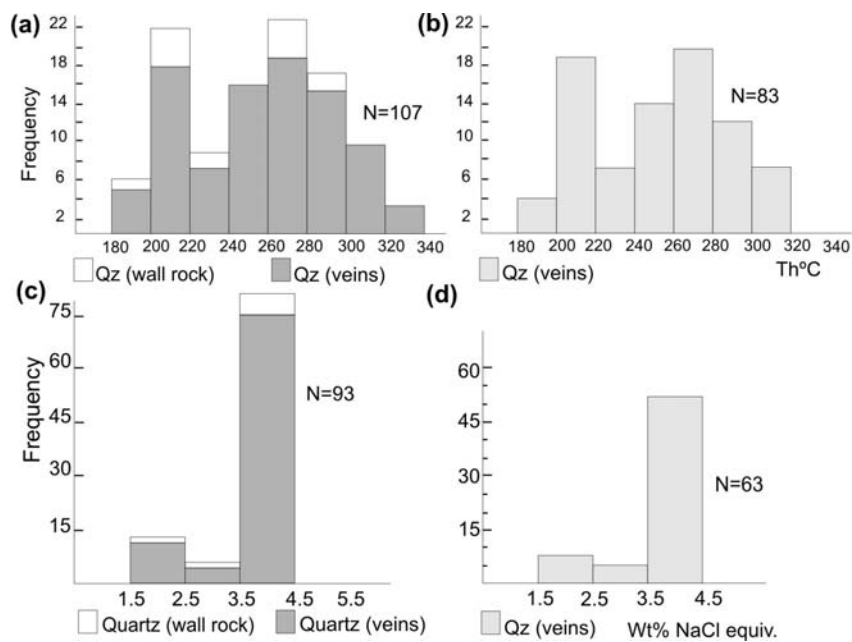


Fig. 8 Histograms of thermometric data for phase changes observed in FI in quartz: Homogenization temperature of L-V inclusions from Lote 15 (a), and Mina de Plomo (b); salinity of aqueous inclusions from Lote 15 (c), and Mina de Plomo (d)

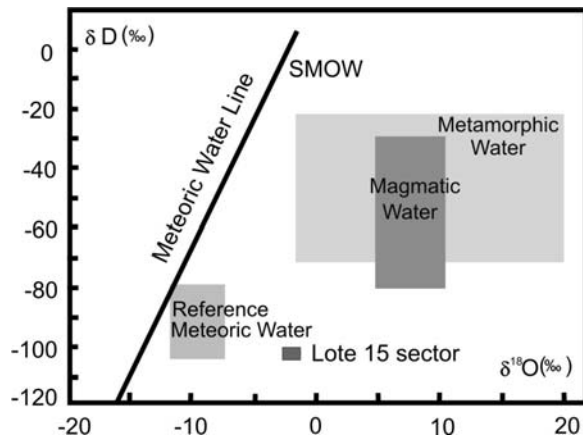


Fig. 9 Stable isotope diagram (δD vs. $\delta^{18}O$) for the Lote 15 sector of Payaniyeu Range (after Sheppard 1986)

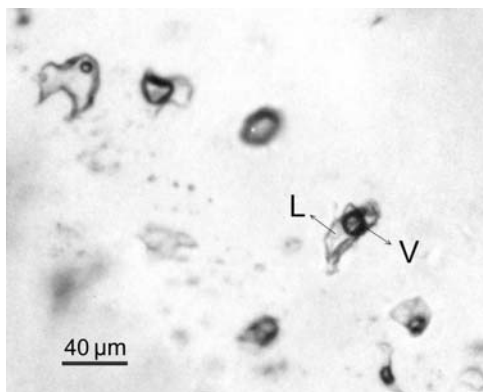


Fig. 10 FI showing boiling indirect evidences, that are based on some groups of primary FI with different proportions of vapor phase that homogenized at the same temperature

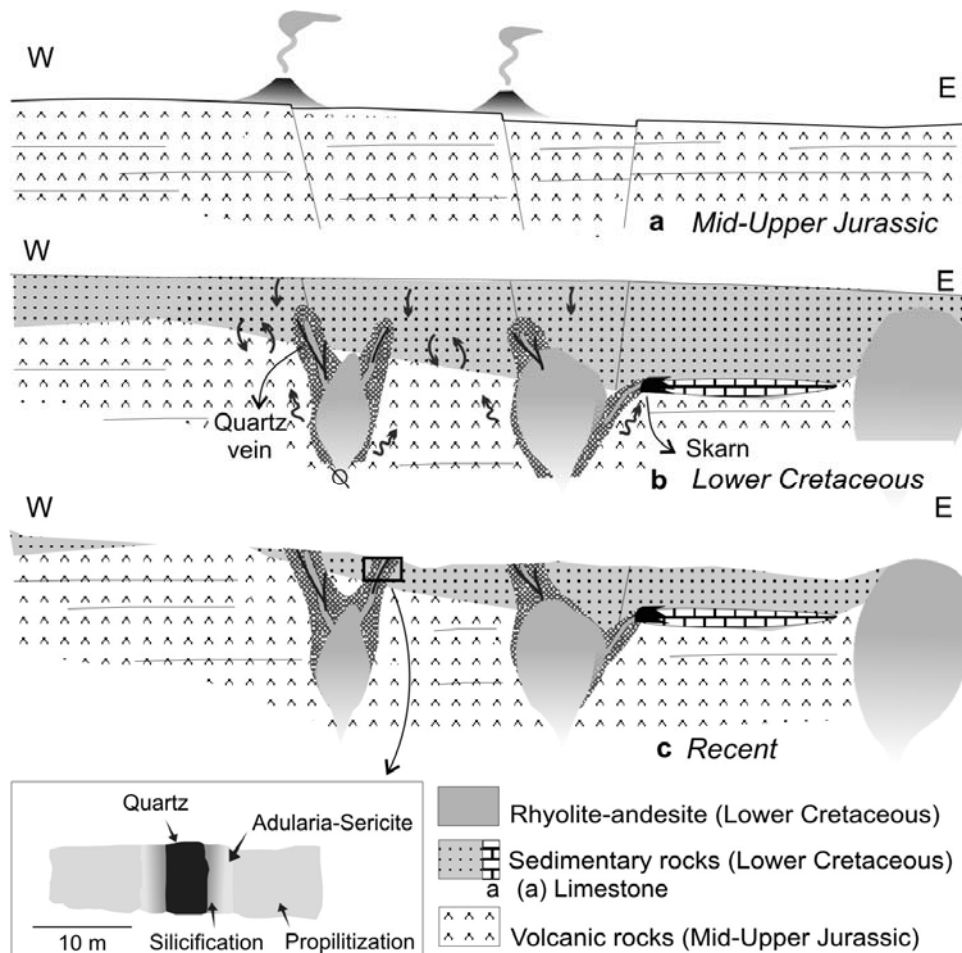


Fig. 11 Schematic cross sections illustrating the metallogenic evolution at Fontana Lake area during the Mid-Upper Jurassic to Lower Cretaceous (not to scale). (a) Mid-Upper Jurassic: The development of an extended basaltic (Lago La Plata Formation) plateau formed a calc-alkaline volcanic arc of N-S trend. (b) Lower Cretaceous: After the volcano sedimentary sequence formation the emplacement of Lower Cretaceous rhyolitic bodies and related quartz veins occurred, together with a skarn formation related to thin interbedded limestone. Arrows denote fluid flow patterns (mixing of magmatic and meteoric waters?) and crossed circle the heat source (c) After a long period of denudation the vein deposits is exposed.

Table 1 Variations in geochemical analyses of main quartz veins from Lote 15, Mina de Plomo, Payaniyeu Range, Del Finadito and Teta Hills, Western Patagonia Argentina.

Quartz veins and veinlets		Au (ppb)	Ag (ppm)	Cu (ppm)	Pb (ppm)	Zn (ppm)	Fe (pct.)	As (ppm)	Sb (ppm)	Hg (ppb)
Lote 15 (N: 24)	Average	340.1	4.9	775.1	2994.8	461.6	4.6	92.5	5.7	1.3
	Max. value	5728.0	26.5	4549.0	16200	1950.0	16.3	380.0	42.6	4.0
	Min. value	6.0	0.1	11.0	65.0	21.0	0.5	4.6	1.7	0.0
Mina de Plomo (N: 10)	Average	691.8	120.7	803.6	22751	351.4	6.2	184.4	13.6	51.0
	Max. value	1560.0	223.8	1180.0	46633	648.0	11.9	429.0	46.0	110.0
	Min. value	5.0	0.3	12.0	128.0	34.0	0.6	2.0	2.0	10.0
Seco Stream (N: 6)	Average	46.8	5.7	5.0	20.8	81.3	1.7	33.7	2.5	0.0
	Max. value	107.0	17.0	7.0	54.0	126.0	2.5	82.0	2.5	0.0
	Min. value	2.5	0.1	3.0	2.3	19.0	1.3	5.0	2.5	0.0
Del Finadito Hill (N: 10)	Average	5.0	0.5	23.8	98.4	94.4	1.3	23.8	2.3	21.0
	Max. value	5.0	0.9	59.0	199.0	189.0	3.1	79.0	3.0	35.0
	Min. value	5.0	0.3	2.0	5.0	3.0	0.1	2.0	2.0	10.0
Teta Hill (N: 13)	Average	124.0	9.0	39.6	30.5	30.1	1.1	38.3	4.3	0.0
	Max. value	524.0	76.5	162.0	84.0	69.0	1.9	112.0	6.0	0.1
	Min. value	2.5	0.1	7.0	7.0	10.0	0.4	2.5	2.5	0.0

Notes: Analytical data supplied by Actlabs Ltd., Canada.

Table 2 Primary fluid inclusion microthermometric data in quartz grains from representative veins at Lote 15, and Mina de Plomo.

Location	Type of mineralization	Origin of inclusion	Th (L+V)	Te	Tm	Salinity
Lote 15	Quartz vein	Primary	180-325	<-24	-2.5/-1.0	1.7/4.8
	Quartz veinlet-wall rock	Primary	180-290	<-23	-2.3/-1.0	1.7/3.8
Mina de Plomo	Quartz vein	Primary	190-310	<-22	-2.4/-1.1	1,9/4.0

Notes: Temperatures are °C units: Th (L+V) homogenization temperature of vapor phase; Td: decrepitation temperature; Te: eutectic temperature; Tm: melting temperature of ice. Salinities (wt % NaCl equiv.) are calculated from ice-melting temperatures.

Table 3 Stable Isotope data from Lote 15, Pepita Hill (El Abuelo skarn and El Solcito vein), and Mina de Plomo sectors.

Sample	Location	Mineral	$\delta^{18}\text{O}_{\text{min}}$ (‰)	$\delta^{18}\text{O}_{\text{H}_2\text{O}}$ (‰)	$\delta\text{D}_{\text{min}}$ (‰)	$\delta\text{D}_{\text{H}_2\text{O}}$ (‰)
L15 1	Lote 15 sector	Quartz	5.3	-2.43		
L15 2	Lote 15 sector	Quartz	5.4	-2.33		
L15 11	Lote 15 sector	Quartz (FI)		-2.85		-106.4
L15 21	Lote 15 sector	Quartz (FI)		-0.91		-103.4
			$\delta^{34}\text{S}_{\text{min}}$ (‰)		$\delta^{34}\text{S}_{\text{H}_2\text{S}}$ (‰)	
P8	Lote 15 sector	Galena	-1.14			0.78
1187	Mina de Plomo	Galena	-1.90			0.02
P8	Lote 15 sector	Pyrite	1.56			0.34
1187	Mina de Plomo	Pyrite	-0.10			-1.32
4231*	El Abuelo skarn	Pyrite	0.1			-1.21
4247*	El Solcito Vein	Pyrite	0.2			-1.20

Notes:

*Data from Lanfranchini et al. (2007)